K_0 Static and Dynamic for a Slanted Wall with a Ramp

By Farid A. Chouery[1], P.E., S.E.

Abstract

Based on classical methods, this paper addresses a theoretical solution to the problem of the static and dynamic pressures on a non-yielding slanted wall with a ramp on top, in sand. First, it derives K_{0r}, the static at rest coefficient for a vertical non-yielding wall with a ramp on top, then for K_{0s} for a slanted non-yielding wall. Additionally, it addresses overconsolidation of sand for these conditions. Second, it gives a theoretical solution for the dynamic at rest coefficient based on Mononobe-Okabe's method. It successfully compares the dynamic solution with the empirical methods and experiments including overconsolidation. These experiments were tested for a vertical wall with a flat surface on top. The results match experiments very closely but show the empirical equation that has been in existence is inappropriate. Finally, it addresses the design of a non-yielding retaining wall based on tolerable lateral displacement. The solution is consistent with the classical methods and offers a wide variety of application in practice.

Introduction

In practice, a non-yielding wall with a ramp on top is very common in sites where there is

[1]Structural, Electrical and Foundation Engineer, FAC Systems Inc., 6738 19th Ave. NW, Seattle, WA

a slope. These types of walls are usually stiff walls or basement walls. Occasionally, there are retaining walls that need to be restricted to yield due to adjacent buried structure, utilities, or footings on the slope. They all need to be designed to a non-yielding wall by using the at rest forces. There has been no theoretical solution given for such conditions. Similarly, a non-yielding slanted wall with a ramp on top has no theoretical solution. Solutions to these problems are important for understanding the forces induced by earthquake as has been demonstrated by Mononobe-Okabe (1929 & 1924)[6,7] for active and passive pressure on sand. Active and passive solutions for a slanted wall with ramp on top were essential in Mononobe-Okabe's equations. The lack of answer to these problems causes the engineer to take unnecessary risks in predicting the pressures on a non-yielding wall. K_0 , the at rest coefficient, static and dynamic is desired to be derived for these conditions. For example: basement walls, stiff walls, abutments, caissons, rigid frames, permanent shoring, tunnels, buried structures etc. requires K_0 static and dynamic with understanding beyond the empirical solutions.

In static conditions, prior work has been developed by the author Chouery [2] in deriving K_0 for a vertical wall with a flat surface on top. The work was done for sand and clay and over-consolidation sand and clay. For a wall slanted inward with a flat surface on top, a solution can be found in textbooks see ref. [12]. In dynamics, for a vertical wall with a flat surface on top, prior experiments in sand has been done by Ichihara, and Matsuzawa (1973)[4] and Sherif et al. (1982)[11]. Ichihara, and Matsuzawa gave empirical expressions for their findings. Sherif et al. showed that the available dynamic elastic solution proposed by Matsuo, and Ohara (1960)[5] and Wood (1973)[13] overestimate by

considerable amount the incremental dynamic stresses against non-yielding retaining structures.

In this paper a theoretical solution is derived for K_0 static based on approximation methods followed by an exact solution. Furthermore, the dynamic equations are presented including over-consolidation and compared with experiments. Finally, the design of a non-yielding retaining wall based on tolerable lateral displacement is addressed.

Static K_0 for a non-yielding vertical wall with a ramp on top

Chouery [2] developed a method to obtain K_0 for a non-yielding vertical wall with a flat surface on top. This method can be extended to derive K_0 for a non-yielding vertical wall with a ramp on top. Starting with the wall with a ramp shown on Fig. 1, where the wall is shown with its mirror image wall, the at rest horizontal force E_{0r} can be obtained by the use of the incipient shear T. The incipient shear was first introduced by Chouery [2] in deriving K_0 . It is a downward shear that is introduced on the boundary and does not change E_{0r} but causes an active failure surface. Consequently, if maximizing E_{0r} with an unknown T through an active slip failure surface, K_0 can be extracted.
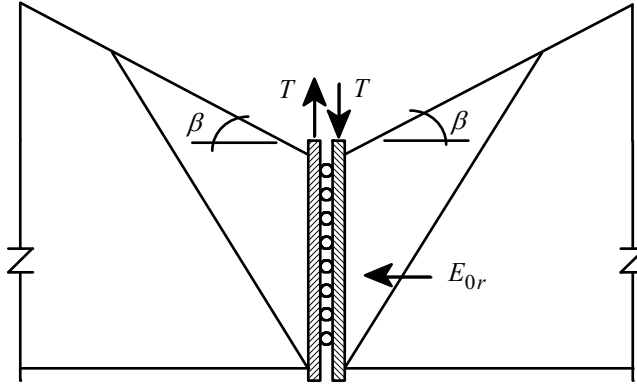
FIG. 1 - Incipient Shear on two sliding walls

a - <u>Boundary Condition</u>

Subdividing the failure wedge of the downward incipient shear into vertical slices following Bishop (1955)[1], yields slices that are in equilibrium. Each slice is added together to make the wedge of Fig. 2(b). The resultant of the boundary forces on a slice can be transformed to a Coulomb (1776)[3] wedge as shown in Fig. 2(a).

From the forces in Fig. 2(a)

$$dE_x = \frac{\gamma(y + x \tan \beta)dx \tan(\alpha - \phi)}{1 + \tan \delta \tan(\alpha - \phi)}$$ .... (1)

Where ϕ is the angle of internal friction of soil, γ is the soil unit weight, and $\tan \delta = dE_y / dE_x$. Solving for $-dE_y$, yields

$$-dE_y = -\gamma(y + x \tan \beta)dx + dE_x \cot(\alpha - \phi)$$ .... (2)

To find α_0 and α_m at the boundary $-dE_y$ needs to be minimized at the boundary.

Substituting $dE_x = K_{0r}\gamma y d\overline{y} = K_{0r}\gamma y(\tan\alpha - \tan\beta)dx$ in Eq. 2, where K_{0r} is the at rest
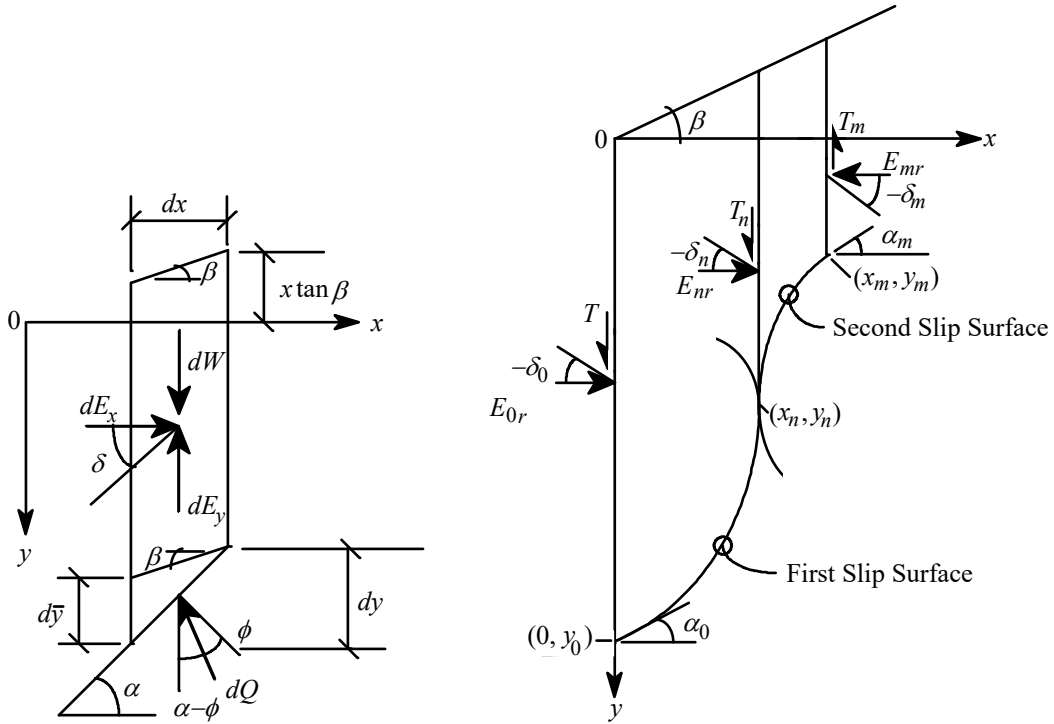

FIG. 2(a) - Coulomb Wedge in a Slice   FIG. 2(b) - Slip Surface

coefficient for a vertical wall with a ramp, and minimizing $-dE_y$ in Eq. 2 with respect to α

, yields

$$\tan\alpha_0 = \tan\alpha_m = \tan\alpha = \tan\phi + \frac{1}{\cos\phi}\sqrt{1-\cot\phi\tan\beta} \quad\text{... (3)}$$

5

Thus, the boundary conditions are obtained.

b - Approximate Solution using a line

Chouery [2] showed that for $\beta = 0$ a line approximation for a failure surface is adequate provided an appropriate safety factor is used. In the case of a wall with a ramp on top the variation between the exact and the approximate ranges from 0 to 10%, where the exact solution will be presented afterwards. For $30 < \phi < 45$ degrees the safety factor can be taken as 9.3%. The need for approximation is to give a simpler equation for K_{0r}. This will become evident later.

Making a change of variable in Eq. 1: $u = y + x \tan \beta$, $du = dy + dx \tan \beta =$

$(-\tan \alpha + \tan \beta)dx$, $u_0 = y_0$, $u_m = y_m + x_m \tan \beta = 0$, and integrating from u_0 to u_m, yields

$$E_{0r} = K_{0r}\gamma \frac{y_0^2}{2} \cong \int_{y_0}^{0} dE_x = \frac{\tan(\alpha - \phi)}{(\tan \alpha - \tan \beta)[1 - \tan \phi \tan(\alpha - \phi)]} \gamma \frac{y_0^2}{2} \text{............................} (4)$$

Where δ was replaces by $-\phi$ for maximum value of dE_x in Eq. 1, and $-\tan\alpha$ is considered a constant since it's the slope for the line equation. Rearranging Eq. 4 , yields

$$K_{0r} \cong \frac{\tan \alpha - \tan \phi}{\tan \alpha - \tan \beta}\cos^2 \phi \text{...} (5)$$

Substituting α from Eq. 3 into Eq. 5, yields the at rest coefficient:

$$K_{0r} \cong \frac{\cos^2 \phi}{1 + \sin \phi \sqrt{1 - \cot \phi \tan \beta}} \quad \text{...} \quad (6)$$

Eq. 6 gives a simple equation.

c - Exact Solution

The exact solution can be obtained by similar methods as in deriving K_0 for a wall with a flat surface on top see Chouery [2]. Therefore, maximizing the horizontal force in the slice, dE_x in Eq. 1, with respect to α, after replacing dx by $-d\overline{y}/(\tan \alpha - \tan \beta)$, yields

$$\tan \delta = \left[\left(\frac{\cos \alpha}{\cos(\alpha - \phi)} \right)^2 \frac{\tan \alpha - \tan \beta}{\tan(\alpha - \phi)} - 1 \right] \frac{1}{\tan(\alpha - \phi)} \quad \text{....................................} \quad (7)$$

Substituting $\tan \delta$ back in Eq. 1 and replacing $\tan \alpha$ by $-y' = -dy/dx$, yields

$$dE_x = \gamma(y + x \tan \beta)dx \left[\frac{-\sin^2 \phi(y' \cot \phi + 1)^2}{y' + \tan \beta} \right] \quad \text{...} \quad (8)$$

and thus

$$dE_y = dE_x \tan \delta = \gamma(y + x \tan \beta)dx \left[1 + \frac{\sin^2 \phi(y' \cot \phi + 1)(y' - \cot \phi)}{y' + \tan \beta} \right] \quad \text{........................} \quad (9)$$

Making a change of variable, $u = y + x \tan \beta$, thus, $u' = y' + \tan \beta$, $u_0 = y_0$,

$u_n = y_n + x_n \tan \beta$, and $u_m = y_m + x_m \tan \beta$, and substitute in Eq. 8 and 9 yields

7

$$dE_x = \gamma u dx \left[\frac{-\sin^2 \phi (u' \cot \phi + 1 - \cot \phi \tan \beta)^2}{u'} \right] \quad \text{.......................................} \quad (10)$$

$$dE_y = \gamma u dx \left[1 + \frac{\sin^2 \phi (u' \cot \phi + 1 - \cot \phi \tan \beta)(u' - \tan \beta - \cot \phi)}{u'} \right] \text{.............................} (11)$$

Maximizing, using variational analysis, on $E_{0r} = \int_0^{x_n} dE_x + E_{nr}$ and $T_n = \int_{x_n}^{x_m} dE_y + T_m$ in

Eq. 10 and 11, yields the two slip surface equations:

$$\frac{1}{u'} = \frac{1}{\tan \beta - \tan \phi} \left(1 - \frac{u_n}{u} \right) \quad \text{...} \quad (12)$$

and

$$\frac{1}{u'} = \frac{1}{\tan \beta + \cot \phi} \left(1 - \frac{u_n}{u} \right) \quad \text{...} \quad (13)$$

Imposing the boundary condition from Eq. 3 at $x = 0$ and at $x = x_m$ along with

$u' = -\tan \alpha + \tan \beta$, yields

$$\frac{u_n}{u_0} = 1 - \frac{\tan \beta - \tan \phi}{\tan \beta - \tan \phi - \dfrac{1}{\cos \phi} \sqrt{1 - \cot \phi \tan \beta}} \quad \text{...} \quad (14)$$

and

$$\frac{u_n}{u_m} = 1 - \frac{\tan \beta + \cot \phi}{\tan \beta - \tan \phi - \dfrac{1}{\cos \phi} \sqrt{1 - \cot \phi \tan \beta}} \quad \text{...} \quad (15)$$

From Eq. 12, and 13 the first and second slip surface in terms of x and y are:

$$x = \frac{1}{\tan\beta - \tan\phi}\left[y + x\tan\beta - y_0 - (y_n + x_n\tan\beta)\ln\left|\frac{y + x\tan\beta}{y_0}\right|\right] \quad\text{............................ (16)}$$

and

$$x - x_n = \frac{1}{\tan\beta + \cot\phi}\left[y + x\tan\beta - y_n - x_n\tan\beta - (y_n + x_n\tan\beta)\ln\left|\frac{y + x\tan\beta}{y_n + x_n\tan\beta}\right|\right] \quad\text{.... (17)}$$

Eq. 16 and 17 involves x and y explicitly. However, they can be handled efficiently by rotating the axis by an angle $-\beta$.

Substituting u' from Eq. 12 in Eq. 10 and 11, after replacing dx by du / u', and integrate from u_0 to u_n yields $E_{0r} - E_{nr}$ and $T - T_n$. Substituting u' from Eq. 13 in Eq. 10 and 11, after replacing dx by du / u', and integrate u_n to u_m yields $E_{nr} - E_{mr}$ and $T_n - T_m$. Then, adding each of the integration to the corresponding horizontal and vertical forces yields $E_{0r} - E_{mr}$ and $T - T_m$. Solving for K_{0r} and $\tan\delta_0$, where

$$E_{0r} - E_{mr} = 0.5(u_0^2 - u_m^2)K_{0r} \quad\text{and}\quad T - T_m = 0.5(u_0^2 - u_m^2)K_{0r}\tan\delta_0 \text{, yields}$$

$$K_{0r} = \frac{\cos^2\phi}{z_0^2 - z_m^2}\left[A_1(1 - z_m^2) - 4A_2(1 - z_m) + 2\ln z_0 - 2A_3\ln z_m\right] \quad\text{................................. (18)}$$

where

$$A_1 = \left[1 + \tan(\phi - \beta)\tan\phi\right]^2,$$

$A_2 = \tan\phi\tan(\phi-\beta)\left[1+\tan(\phi-\beta)\tan\phi\right]$,

$A_3 = \tan^2\phi\tan^2(\phi-\beta)$,

$z_0 = 1+\sin\phi\sqrt{1-\cot\phi\tan\beta}$, and

$z_m = \sin\phi\sqrt{1-\cot\phi\tan\beta}$.

The incipient shear angle δ_0 can be found from the following:

$$\tan\delta_0 = \tan\delta_m = \frac{B_1(z_0^2-1)-4B_1(z_0-1)+2B_2\ln z_0 - B_3(1-z_m^2)-2B_4\ln z_m}{(z_0^2-z_m^2)K_{0r}} \quad \text{......... (19)}$$

where

$B_1 = \cos^2\phi\left[\tan\phi+\cot(\phi-\beta)\right]$,

$B_2 = \cos^2\phi\cot(\phi-\beta)$,

$B_3 = \sin^2\phi\left[\cot\phi+\tan(\phi-\beta)\right]$, and

$B_4 = \sin^2\phi\tan(\phi-\beta)$.

ϕ	β									
	-5	-10	-15	-20	-25	-30	-35	-40	-45	-50
0	1.000	1.000	1.000	1.000	1.000	1.000	1.000	1.000	1.000	1.000
5	0.951	0.934	0.918	0.904	0.889	0.875	0.860	0.844	0.828	0.810
10	0.874	0.851	0.831	0.811	0.792	0.774	0.755	0.736	0.715	0.693
15	0.784	0.761	0.740	0.720	0.700	0.681	0.662	0.642	0.622	0.600
20	0.691	0.670	0.650	0.631	0.613	0.595	0.577	0.559	0.540	0.519
25	0.599	0.581	0.564	0.547	0.531	0.515	0.499	0.483	0.466	0.448
30	0.512	0.496	0.482	0.468	0.454	0.441	0.427	0.413	0.399	0.383
35	0.430	0.417	0.406	0.395	0.384	0.373	0.361	0.350	0.338	0.324
40	0.355	0.345	0.336	0.327	0.319	0.310	0.301	0.292	0.282	0.271
45	0.287	0.279	0.273	0.266	0.259	0.253	0.246	0.239	0.231	0.223
50	0.226	0.221	0.216	0.211	0.206	0.201	0.196	0.191	0.185	0.179

TABLE - 1 K_{0r} values for ϕ and negative β values.

The dividing line shown is to distinguish the values for $-\beta > \phi$

ϕ	β									
	0	5	10	15	20	25	30	35	40	45
0	1.000									
5	0.969	0.992								
10	0.899	0.929	0.970							
15	0.810	0.840	0.878	0.933						
20	0.715	0.742	0.775	0.817	0.883					
25	0.620	0.643	0.670	0.704	0.748	0.821				
30	0.529	0.547	0.569	0.595	0.627	0.672	0.750			
35	0.443	0.458	0.474	0.494	0.518	0.548	0.591	0.671		
40	0.365	0.376	0.388	0.403	0.420	0.441	0.468	0.508	0.587	
45	0.294	0.302	0.311	0.321	0.333	0.347	0.365	0.389	0.425	0.500
50	0.231	0.237	0.243	0.250	0.258	0.267	0.279	0.293	0.313	0.345

TABLE - 2 K_{0r} values for ϕ and positive β values.

The shear angle δ_n can be found from the following:

$$\tan\delta_n = \frac{-B_1(z_0{}^2 - 1) + 4B_1(z_0 - 1) - 2B_2 \ln z_0 + K_{0r}z_0{}^2 \tan\delta_0}{-2\ln z_0 + K_{0r}z_0{}^2} \quad\text{.................................. (20)}$$

Table 1 and 2 gives values for K_{0r} based on Eq. 18. When comparing with the

approximate Eq. 6 the range of difference can be obtained. Note: the K_{0r} values can be

restricted for $|\beta| \le \phi$, since it is the angle of repose for a sliding mass on a slope. This

can, also , be seen in Eq. 3 ; β cannot be greater than ϕ since it produce a negative value under the square root. However, for $-\beta > \phi$ the equations gives values for K_{0r} as shown above the dividing line in Table 1, These values can be considered if assumed the soil is restrained against movement with a barrier on the slope. Thus, it will keep the soil from sloughing and the deflection at zero. One may encounter similarities in the classic Coulomb equation for active pressure. Also, Note: at $\beta = \phi$ $K_{0r} = \cos^2\phi$. This is the maximum possible value of K_{0r}. If compare with Coulomb, Rankine, and Terzaghi's state active pressure, one finds that: for Coulomb at $\beta = \phi$ the horizontal active coefficient K_{Ah} $= \cos^2\phi$ regardless of the friction on the wall. The failure wedge angle with the horizontal is ϕ, the angle of repose and parallel with the top surface. For Rankine and Terzaghi (log-spiral method) they both give $K_{Ah} = \cos^2\phi$. Even though they all give the same pressure, the at rest condition does not constitute a failure wedge. What it means is when $\beta = \phi$ regardless of the wall movement, to create an active condition, the forces does not change from the at rest condition. This is obvious since the failure wedge angle is the angle of repose. Thus soil becomes a parallelogram mass sliding down on a ramp with an angle ϕ with the horizontal while keeping the at rest pressure.

When comparing with empirical formulas such as the Danish Code (Danish Goetechnical Institute 1978) recommended by The US Army Corps of Engineers [14] we find at $\phi = 30^o$ with $\beta = -10^o$ the proposed values are higher by 20% and lower by 3% at $\beta = +10^o$ and lower by 6.6% at $\beta = +20^o$, see table 3.

ϕ (deg)	$\beta = -10°$		$\beta = 10°$		$\beta = 20°$	
	K_{0r} (Danish) $=$ $(1-\sin\phi)(1+\sin\beta)$	K_{0r} (derived)	K_{0r} (Danish) $=$ $(1-\sin\phi)(1+\sin\beta)$	K_{0r} (derived)	K_{0r} (Danish) $=$ $(1-\sin\phi)(1+\sin\beta)$	K_{0r} (derived)
10	0.683	0.851	0.970	0.970		
15	0.612	0.761	0.870	0.878		
20	0.544	0.670	0.772	0.775	0.883	0.883
25	0.477	0.581	0.678	0.670	0.775	0.748
30	0.413	0.496	0.587	0.569	0.671	0.627
35	0.352	0.417	0.500	0.474	0.572	0.518
40	0.295	0.345	0.419	0.388	0.479	0.420
45	0.242	0.279	0.344	0.311	0.393	0.333

TABLE - 3 Comparison of K_{0r} values with Empirical Formula.

d - Resultant directional angle

If the surface of a half space makes and angle β with the horizontal, then the resultant

pressure on a vertical plane is parallel to the soil surface; these directions are conjugate.

From this observation the resultant becomes $E_r = E_{0r} / \cos\beta$ located at a line parallel to

the surface or intersects the wall with an angle β from the horizontal.

Static K_0 for a non-yielding slanted wall with a ramp on top

When extending the incipient shear method for a slanted wall one may find, while

keeping the wall deflection at zero, an induced shear is required on the wall. Thus, when

applying the incipient shear concept, T gets mixed up with the induced shear and they

cannot be separated in the derivation. Furthermore, in order to keep the forces equal at

the wall for a zero deflection, the mirror image of the wall is not sufficient to do the

work. Consequently, a different β is necessary to use in the mirror image resulting in

unsymmetrical shapes. Symmetry is an essential requirement to execute the incipient

shear method. The incipient shear method for a slanted wall can be used by forcing symmetry of gavity loads and in that case the gravity load is not pointing downwards. The derivation is involved and an alternative method will be used.

Consider the slanted inward and outward walls in Fig. 3(a,b) respectively. In both cases they are assumed to be in the at rest condition. Thus, the deflection is zero at the wall and is assumed zero at any vertical line beyond the walls. Therefore, the solution can be obtained by using the solution in Eq. 6 or 18 for a vertical wall with a ramp on top. However, the solution must be separated into two cases: slanted inward and slanted outward.

a - <u>Static case $\xi > 0$ for a wall slanted inward</u>

Consider the forces in Fig. 3(a), it is found that in order the forces to coincide at the 1/3 point of the wall, there must exist a shear on line a-b with $E_r = E_{0r}(\beta) / \cos\beta$. This is necessary in order to keep the summation of moments at the 1/3 point of the wall equal zero. This makes it consistent with the classical methods and the observation made in paragraph (d) above. Thus, the pressure diagram will remain in a triangular distribution. From the geometry in Fig 3(a) it yields
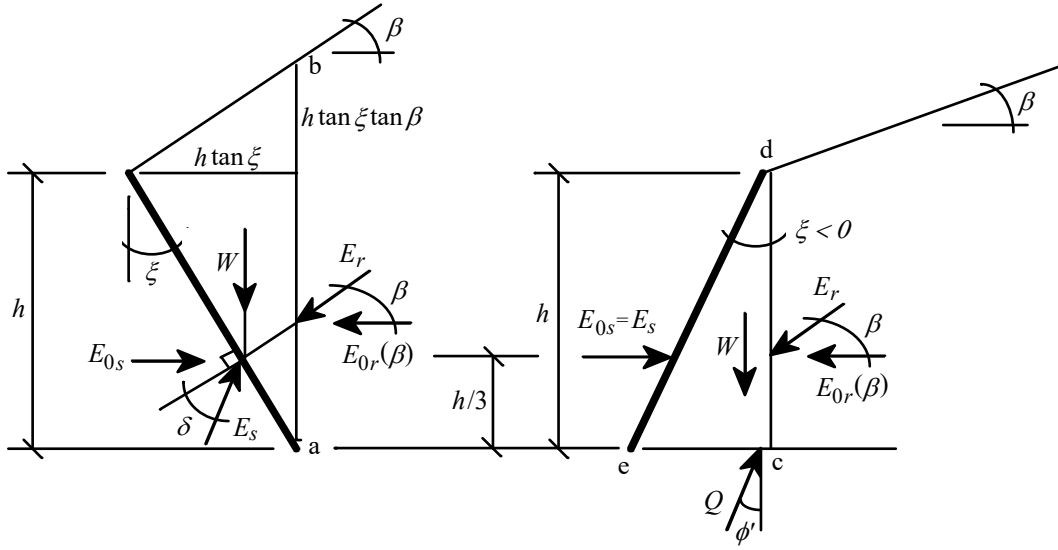
FIG. 3(a) Wall Slanted Inward   FIG. 3(b) Wall slanted outward

$$W = \frac{1}{2}\gamma h^2 \tan\xi(1+\tan\xi\tan\beta) \quad\text{.. (21)}$$

and

$$E_{0r}(\beta) = \frac{1}{2}\gamma h^2 (1+\tan\xi\tan\beta)^2 K_{0r}(\beta) \quad\text{... (22)}$$

where $K_{0r}(\beta)$ is the same as K_{0r} in Eq. 6 or 18. It is shown as a function of β to simplify

substituting for β different variables. From the force diagram the resultant becomes:

$$E_s = \sqrt{\left[E_{0r}(\beta)\right]^2 + \left[W+\tan\beta\, E_{0r}(\beta)\right]^2} \quad\text{... (23)}$$

and

$$\tan\delta = \frac{\cos\xi\left[W + \tan\beta\, E_{0r}(\beta)\right] - \sin\xi\, E_{0r}(\beta)}{\sin\xi\left[W + \tan\beta\, E_{0r}(\beta)\right] + \cos\xi\, E_{0r}(\beta)}$$

$$= \frac{\tan\xi - (\tan\xi - \tan\beta)(1 + \tan\xi\tan\beta)K_{0r}(\beta)}{\tan^2\xi + (1 + \tan\xi\tan\beta)^2 K_{0r}(\beta)} \quad\text{.. (24)}$$

where δ is the directional angle to a line perpendicular to the wall. The horizontal force can be obtained as

$$E_{0s} = E_s\cos(\delta + \xi) = \frac{1}{2}\gamma h^2 (1 + \tan\xi\tan\beta)^2 K_{0r}(\beta) \quad\text{.................................... (25)}$$

Thus, the at rest horizontal coefficient for a wall slanted inward with a ramp on top becomes

$$K_{0s} = (1 + \tan\xi\tan\beta)^2 K_{0r}(\beta) \quad\text{... (26)}$$

b - Static case $\xi < 0$ for a wall slanted outward

Consider the forces in Fig. 3(b), if the resultant force, that is coming beyond line c-b, is causing a vertical component, $E_{0r}(\beta)\tan\beta$, and a moment then the force Q on line e-c will adjust its magnitude and location to balance the forces and the moments. Thus the at rest resultant force, E_s, on the wall will line up with the horizontal component of the resultant on line c-b and no vertical force gets to be on the wall. In other words the

17

vertical component on line c-b gets dissipated in the soil and none is transferred to the wall. Now, the friction, $Q \tan \phi' = (W + E_{0r}(\beta) \tan \beta) \tan \phi'$, under the wedge edc is not fully mobilized since the at rest condition is considered and ϕ' becomes the immobile internal angle of friction. In fact at $\xi{=}0 \ \tan \phi' = 0$, since the strain is considered zero at point c. On the other hand, at $\xi = -\pi / 2 + \phi$ it gives $E_{0s} = E_{0r} - Q \tan \phi' = 0$. This is true since ξ became the angle of repose for a sliding mass on a slope. It is reasonable to assume the immobile coefficient of friction is linearly proportional to the base length for a unit height, or linearly proportional to the weight of the wedge edc. So, $\tan \phi'$ varies linearly with $\tan \xi$. This can be realized since the change in strain on line e-c will vary with the weight. Thus, from the two known points: at $\tan \xi{=}0 \ \tan \phi'{=}0$, at

$\tan \xi = \tan(-\pi / 2 + \phi) \ E_{0s} = E_{0r} - (W + E_{0r} \tan \beta) \tan \phi' = 0$, with $W = (1/2)h^2 \tan \xi$, and

$E_{0r} = (1/2)h^2 K_{0r}(\beta)$ it yields the equation

$\tan \phi' = -K_{0r}(\beta) \tan \phi \tan \xi / \left[K_{0r}(\beta) \tan \beta + \cot \phi \right]$. Substituting back in E_{0s} yields

$$E_{0s} = E_s = \frac{1}{2}\gamma h^2 K_{0r}(\beta) \left[1 + \frac{K_{0r}(\beta) \tan \beta - \tan \xi}{K_{0r}(\beta) \tan \beta + \cot \phi} \tan \phi \tan \xi \right] \quad \text{............................} (27)$$

Thus, the at rest horizontal coefficient for a wall slanted outward with a ramp on top becomes

$$K_{0s} = K_{0r}(\beta) \left[1 + \frac{K_{0r}(\beta) \tan \beta - \tan \xi}{K_{0r}(\beta) \tan \beta + \cot \phi} \tan \phi \tan \xi \right] \quad \text{......................................} (28)$$

The directional angle of the resultant E_s relative to a line perpendicular to the wall is ξ, and ξ is less than zero, coinciding with the horizontal component E_{0s}. Note: not all values of β makes $\phi' \leq \phi$. However, the inequality is true for a very wide range approximately $-0.4\pi \leq \beta \leq \phi$ using $\xi = -\pi/2 + \phi$ as the maximum value.

c - Pressure diagram

Since the forces coincide at the 1/3 point of the wall in Fig 3(a,b), the pressure can be assumed practically universal at full scale. Thus, the pressure diagram is defined by the at rest coefficient acting in a triangular pressure distribution with the center of pressure at 0.33h.

Effect of overconsolidation of sand

Sherif et al. (1984) [10] obtained experimentally the additive term to K_0 due to overconsolidation. Their experiment was done on a vertical wall with a flat surface on top and the resulting additive term to K_0 is: $5.5\left(\gamma_D / \gamma_L - 1\right)$, where γ_D is the dense unit weight at rebound or actual and γ_L is the loose unit weight of soil. Chouery [2] confirmed theoretically the findings. He adjusted the overconsolidation factor to 5.87 instead of 5.5. This was necessary to account for the real K_0 derivation and using γ_L instead of γ_D in calculating the at rest force and the stress. In general, locked-in stresses can only endure in the horizontal direction. Thus, in the case of a slanted wall with a ramp on top the additive term is added to the horizontal at rest coefficient. Consequently, $K_{0r}(\beta)$ in Eq. 22, 24, 25, 26, 27, and 28, is to be replaced by $K_{0r,oc}(\beta)$ where

$$K_{0r,oc}(\beta) = K_{0r}(\beta) + 5.87\left(\frac{\gamma_D}{\gamma_L} - 1\right)$$ .... (29)

Additionally, γ in Eq. 21, 22, 25, and 27, is to be replace by γ_L, and replace ϕ by ϕ_L where it is based on the loosest state.

At rest coefficient under earthquake

In the earthquake resistant design of retaining walls, the earth pressure caused by an active condition against the wall is calculated by Mononobe-Okabe (1929 & 1924)[6,7] equation. Ichihara, and Matsuzawa (1973)[4] and Sherif et al. (1982)[11] showed that the Mononobe-Okabe equation is adequate with the angle of friction is fully mobilized for the maximum inertia force. Additional, the angle of wall friction $\delta \cong (1/2)\phi$ or δ_{max} . However, the wall is assumed to move sufficiently before excitation to develop the corresponding active triangular distribution pressure. Much research and experiments has been done in that area confirming Mononobe-Okabe's equation. For a non-yielding wall, the friction has minimal effect on the forces since the relative deflection between the wall and soil is considered zero. This is expected since the wall and the soil moves together in an earthquake. When following Mononobe-Okabe's derivation: $\theta = \tan^{-1}\left[k_h / (1 - k_v)\right]$ where k_h and k_v are the horizontal and vertical acceleration coefficients. Then, γ becomes $\gamma(1 - k_v)/\cos\theta$, h becomes $h\cos(\xi + \theta)/\cos\xi$, and the earthquake parameters are as follows:

a - Dynamic case $\xi + \theta > 0$ for a wall slanted inward

The maximum and minimum forces and coefficients can be obtained from:

$$E_{0sE} = \frac{1}{2}\gamma h^2 (1 - k_v) K_{0sE} \quad\text{...} \quad (30)$$

$$K_{0sE} = \frac{\cos^2(\xi + \theta)}{\cos^2 \xi \cos \theta}[1 + \tan(\xi + \theta)\tan(\beta + \theta)]^2 K_{0r}(\beta + \theta) \quad\text{..........................} \quad (31)$$

$$V_{0sE} = \frac{1}{2}\gamma h^2 (1 - k_v) K_{0sEv} \quad\text{...} \quad (32)$$

$$K_{0sEv} = \frac{\cos^2(\xi + \theta)}{\cos \xi \cos \theta}\left\{\tan(\xi + \theta)[1 + \tan(\xi + \theta)\tan(\beta + \theta)] + \tan(\beta + \theta)[1 + \tan(\xi + \theta)\tan(\beta + \theta)]^2 K_{0r}(\beta + \theta)\right\}$$

$$\text{..} \quad (33)$$

$$E_{sE} = \sqrt{(E_{0sE})^2 + (V_{0sE})^2} \quad\text{...} \quad (34)$$

$$\tan \delta_E = \frac{V_{0sE}\cos\xi - E_{0sE}\sin\xi}{V_{0sE}\sin\xi + E_{0sE}\cos\xi} \quad\text{...} \quad (35)$$

where E_{0sE} is the horizontal earthquake force on the wall, K_{0sE} is the horizontal coefficient of seismic earth pressure at rest, V_{0sE} is the vertical earthquake force on the wall, K_{0sEv} is the vertical coefficient of seismic earth pressure at rest, E_{sE} is the resultant earthquake force on the wall, and δ_E is the directional angle of the resultant relative to a line perpendicular to the wall at initial state.

b - <u>Dynamic case $\xi + \theta < 0$ for a wall slanted outward</u>

The maximum and minimum forces and coefficients can be obtained from:

$$E_{0sE} = E_{sE} = \frac{1}{2}\gamma h^2 (1-k_v)K_{0sE} \quad \text{..} \quad (36)$$

$$K_{0sE} = K_{0r}(\beta+\theta)\left[1 + \frac{K_{0r}(\beta+\theta)\tan(\beta+\theta) - \tan(\xi+\theta)}{K_{0r}(\beta+\theta)\tan(\beta+\theta) + \cot\phi}\tan\phi\tan(\xi+\theta)\right]\frac{\cos^2(\xi+\theta)}{\cos^2\xi\cos\theta}$$

$$\text{..} \quad (37)$$

c - <u>Dynamic case $\xi + |\theta| > 0$ and $\xi - |\theta| < 0$</u>

This condition normally happens for a vertical wall with $\xi = 0$ with $\pm|\theta|$. In any case the solution for maximum forces can be found from case (a) above for $\xi + |\theta| > 0$, and for minimum forces it can be found from case (b) above for $\xi - |\theta| < 0$.

d - <u>Location of the line of action of the resultant earthquake force</u>

Seed and Whitman (1970)[9] proposed a simple procedure to determine the location of the line of action of the resultant in an active condition. This procedure can also be adapted for a non-yielding wall. Ichihara, and Matsuzawa (1973)[4] gave an empirical expression for the location of the resultant for a vertical wall with flat surface on top. Their result shows the location varies from 1/3 to 0.38h depending on θ where $0 \leq \tan\theta \leq 0.57$. Sherif et al. (1982)[11] showed the location to be at 0.4h for the maximum resultant and 0.52h for the maximum incremental dynamic neutral earth thrust. Because the resultant location will vary depending on the amount of wall movement and the way in which the movement occurs, it is not simple to derive a theoretical expression. It seems that the empirical methods are preferred. However, since the location of the

resultant is taken relative to the initial state, then it can be taken as

$[1 - 0.67 \cos(\xi + \theta)/\cos\xi]h$. This expression is derived from projecting a line horizontally

from the 1/3-point at $\xi + \theta$ inward inclination of the wall to the vertical line. For $\xi = 0$ it

gives $(1 - 0.67\cos\theta)h$ or 0.42 at $\tan\theta = 0.57$. This Equation is slightly higher than

Ichihara and Matsuzawa's curve but accurate with Sherif et al. at $\tan\theta = 0.5$. Based on

this recommendation the incremental dynamic neutral thrust must adjust correspondingly.

Comparison with experiments

Ichihara, and Matsuzawa (1973)[4] showed, for a vertical wall with a flat surface on top,

the horizontal maximum earth force at rest can be calculated by the empirical equation

$$E_{0sE}\Big|_{\xi=\beta=0} \cong \frac{1}{2}\gamma h^2\left[K_0 + \frac{1}{2}(K_{AE} - K_A)\right] \dots\dots\dots (38)$$

where K_{AE} is the coefficient of horizontal active pressure during an earthquake

(Mononobe-Okabe' equation), K_A is the active horizontal coefficient at static (Coulomb's

equation) and both K_{AE} and K_A is calculated at $\delta = (1/2)\phi$, and K_0 is 1-$\sin\phi$. The friction

angle of soil used in the experiment was $\phi = 42$ degrees $\gamma = 1.59$ gm/cm³ for Toyoura

Sand. The measured K_0 is much higher than 1-$\sin\phi$ due to overconsolidation by shaking.

Note: Their definition of Eq. 38 is the resultant earth pressure at the maximum inertia

force related to K_{0max} as described by their Fig. 19. However, Eq. 3 of their paper defines

K as the horizontal coefficient as it is used in their Fig. 13 and 14. Consequently, This

interprets Eq. 38 to be the horizontal force at rest instead of the resultant. Therefore, Eq.

38 is to be compared with Eq. 30 against different ϕ values. Fig. 4 shows the difference

between the normalized horizontal [normalized to $(1/2)\gamma h^2$] in Eq. 30 minus Eq. 38 for ϕ = 30 and 42 degrees verses k_h with $k_v = 0$.

The result shows, in the tested range $0 < k_h < 0.38$, that Eq. 30 fits the empirical Eq. 38 at $\phi = 42$ degrees better than at $\phi = 30$ degrees. This is expected since Eq. 38 was derived for $\phi = 42$ degrees showing -1% to 3.3% variations in magnitude. However, it seems that Ichihara, and Matsuzawa's empirical Eq. 38 is not applicable since it underestimates the horizontal force by 0 to 17.2% in magnitude in the full range of k_h. The reason in the discrepancy is maybe the empirical Eq. 38 was obtained for a soil that was under consolidation. Sherif et al. (1982)[11] described the difference in their experiment is due to overconsolidation by shaking. It is found not possible to compare to the actual experiment of Ichihara, and Matsuzawa and include overconsolidation, since the available data are not sufficient to determine ϕ_L and γ_D / γ_L.

When comparing with Sherif et al. (1982)[11] it is necessary to consider overconsolidation. Rewriting Eq. 29 for the case $\xi + \theta > 0$, the horizontal earthquake force becomes:

$$E_{0sE,oc} = \frac{1}{2}\gamma_L h^2 (1-k_v)K_{0sE} + \frac{1}{2}\gamma_L h^2 (1-k_v)\frac{\cos^2(\xi+\theta)}{\cos^2\xi\cos\theta}[1+\tan(\xi+\theta)\tan(\beta+\theta)]^2 (5.87)\left[\frac{\gamma_D}{\gamma_L}-1\right]$$

$$\dots\dots\dots\dots\dots\dots\dots\dots\dots\dots\dots\dots\dots\dots\dots\dots\dots\dots\dots\dots\dots\dots\dots\dots\dots\dots \text{(39)}$$

where K_{0sE} is from Eq. 31, and replace ϕ by ϕ_L where it is based on the loosest state. The horizontal seismic at rest coefficient for overconsolidation becomes:

$$K_{0sE,oc} = K_{0sE} + \frac{\cos^2(\xi+\theta)}{\cos^2\xi\cos\theta}[1+\tan(\xi+\theta)\tan(\beta+\theta)]^2 (5.87)\left[\frac{\gamma_D}{\gamma_L}-1\right] \dots\dots\dots\dots \text{(40)}$$
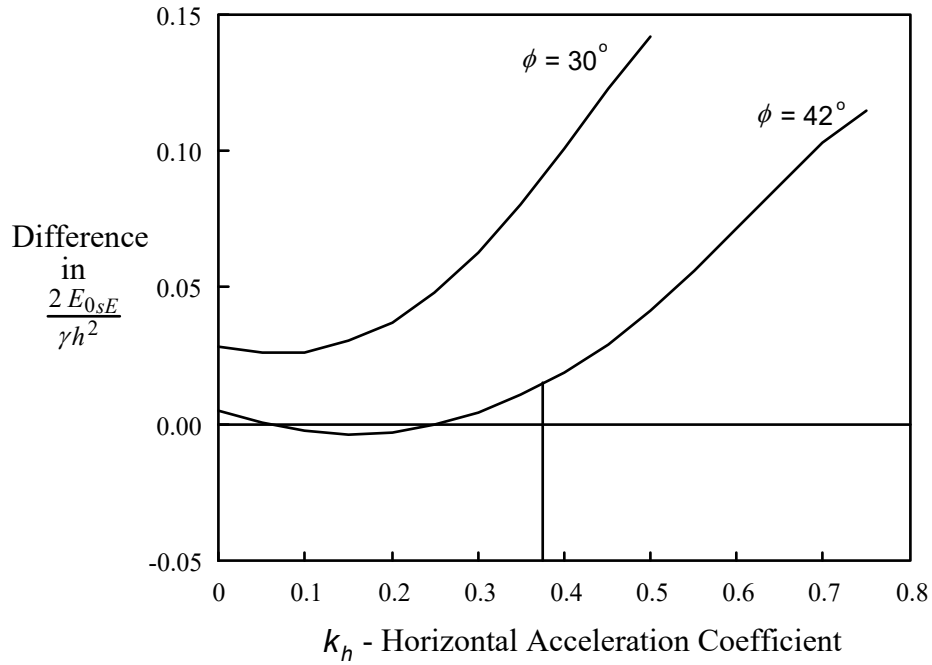
24

FIG. 4 Difference between empirical and derived equations

for a vertical wall with a flat surface on top.

For the case $\xi + \theta > 0$, the term $5.87(\gamma_D / \gamma_L - 1)$ is additive to the term in the bracket in

Eq. 37.

Sherif et al. (1982)[11] results was based on $k_v = 0$, an average soil weight of $\gamma_{ave} = 1.66$

gm/cm³ for Ottawa Silica Sand, and average internal soil friction of $\phi_{ave} = 40.9$ degrees.

In order to compare, it is necessary to find ϕ_L for the loosest state. From their chart, at k_h

$= 0$

$K_{0,oc} = 0.49 = K_0(\phi_L) + 5.87(\gamma_D / \gamma_L - 1)$. Substituting $\gamma_D = \gamma_{ave} = 1.66$ gm/cm³ , and γ_L

from Sherif et al. (1984)[10]: $\gamma_L = 0.0117(\phi_L - 32) + 1.549$ gm/cm³ in $K_{0,oc}$ and calculate

ϕ_L numerically yields $\phi_L = 38.92$ degrees and $\gamma_L = 1.63$ gm/cm^3 . Substituting, $\xi = \beta = 0$,

$\phi = 38.92$ degrees, and the term $5.87\left(\gamma_D / \gamma_L - 1\right) = 0.109$ [i.e. $(K_{0,oc} - K_0) = 0.49 - 0.381$]

in Eq. 40, and comparing the results for different k_h values yields the curves in Fig. 5.

Fig. 5 shows the derived is in good results with experiment. The doted curve is from

Sherif et al. (1982)[11] and is based on best-fit curve to all test data, and was drawn

based on the average density of all test soils. The solid curve is the derived from Eq. 40

and showing slightly lower values for $K_{0sE, oc}$ than the best-fit curve. The maximum

percent variation between experiment minus derived divided by derived, calculates to be

3.7%. For all practical purpose, this is considered a mach.

For the minimum horizontal seismic at rest coefficient for overconsolidation, the

theoretical equations gives lower values than Sherif's et al. (1982)[11] best-fit curve from

experiment (27% lower at maximum point). Selectively, it is shown on Fig. 5 for
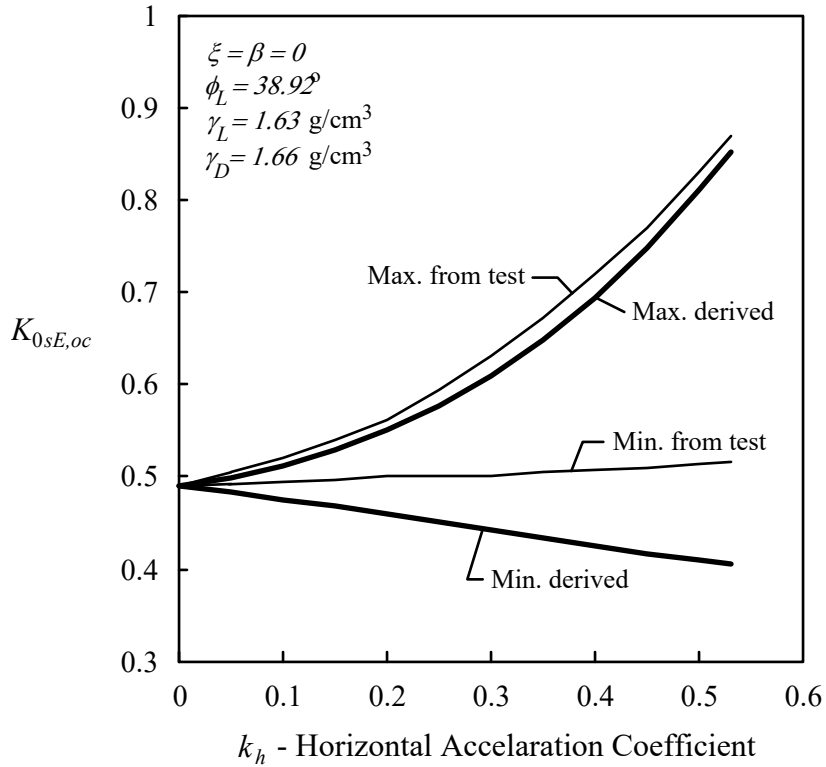
FIG. 5 Horizontal seismic at rest coefficient for overconsolidation

for a vertical wall with a flat surface on top

comparison. Similarly, when using Mononobe-Okabe's equation, the minimum horizontal

thrust does not match experiments. It seems the minimum dynamic thrust does not match

experiment possibly due to not taking into consideration the inertia effect of the wall.

Also, possible impact forces will occur on the down swing of the acceleration, due to

difference in mass between soil wedge and wall. This will cause an increase in the

minimum pressure. Therefore, for the minimum horizontal seismic coefficient, the

experiments will not match the theoretical equations. In any case, the minimum

horizontal seismic coefficient is rarely needed in practice.

Design of a non-yielding retaining wall based on tolerable lateral displacement

It has been shown by several investigators that even under mild earthquake conditions, there is some lateral displacement of retaining wall. For a non-yielding wall these displacements may not effect the at rest pressure itself. If sufficient movement occurs, the pressure becomes an active condition. This off course not acceptable since the design intent was to have an approximate non-yielding wall. Richards and Elms (1979)[8] proposed a procedure for designing gravity retaining walls for earthquake conditions, which allows limited lateral displacement of the walls. This procedure takes into consideration the inertia effect of the wall. In their analysis the active condition was considered based on Mononobe-Okabe's equation. To repeat the analysis for the at rest condition, it is found few modifications are necessary:

$$W_w = C_{IE} E_{sE} \quad\text{.. (41)}$$

$$C_{IE} = \frac{\cos(\delta_E + \xi) - \sin(\delta_E + \xi)\tan\phi_b}{(1 - k_v)(\tan\phi_b - \tan\theta)} \quad \text{for} \quad \xi + \theta \geq 0 \quad\text{................................ (42)}$$

$$C_{IE} = \frac{1}{(1 - k_v)(\tan\phi_b - \tan\theta)} \quad \text{for} \quad \xi + \theta < 0 \quad\text{.. (43)}$$

where W_w is the self-weight of the retaining wall, C_{IE} is the wall inertia factor, ϕ_b is the friction angle between bottom of the wall and the soil on which it is resting, δ_E and E_{sE} is from Eq. 35 and 34 for $\xi + \theta > 0$, and E_{sE} is from Eq. 36 for $\xi + \theta < 0$.

Conclusion

Based on classical methods, a theoretical solution is derived for static and dynamic pressures in sand for a slanted non-yielding wall with a ramp on top, including overconsolidations. Additional, design of a non-yielding retaining wall based on tolerable lateral displacement is addressed. The solution was based on classical methods and only practical assumptions were made. In dynamics, the results were successfully compared with experiments. These experiments were done on small-scale models in the laboratory for a vertical wall with a flat surface on top. The results match experiments very closely but the empirical equation by Ichihara and Matsuzawa (1973)[4] is shown inappropriate. It can underestimate the horizontal at rest force by 17.2%. The solution is consistent, tractable, and offers a wide variety of application in practice.

Acknowledgments

Appendix I.-References

1.   Bishop, A. W. (1955). "The Use of Slip Circle in the Stability Analysis of Slopes," *Géotechnique*, London, England, Vol. 5, No. 1, pp. 7-18.

2.   Chouery, Farid A. "Variational Method in Deriving K_0" a companion paper

www.facsystems.com/prod01.htm

3.   Coulomb, Charles Augustin (1776). "Essai sur une application des règles de maximis et

minimis à quelques problèmes de statique relatifs à l'architecture," *Mem. Div. Savants,*

Acad. Sci., Paris, Vol. 7.

4.   Ichihara, M., and Matsuzawa, H. (1973). "Earth Pressure during Earthquake," *Soils and*

Foundations, Japanese Society of soil Mechanics and Foundation Engineering, Vol. 13,

No. 4.

5.   Matsuo, H., and Ohara, S. (1960). "Lateral Earth Pressures and Stability of Quay Walls

during Earthquakes," *Proceedings of the Second World Conference on Earthquake*

Engineering, Japan, Vol. 1, pp. 165-181

6.   Mononobe, N. (1929). "Earthquake-Proof Construction of Masonary Dams,"

Proceedings of the world Engineering Conference, Vol. 9, p. 275.

7.   Okabe, S. (1924). "General Theory of Earth Pressure," *Journal of Japanese Society of*

Civil Engineers, Tokyo, Japan, Vol. 12, No. 1.

8.   Richards, R., and Elms, D. G. (1979). "Seismic Behavior of Gravity Retaining Walls,"

Journal of the Geotechnical Engineering Division, ASCE, Vol. 105, No. GT4, pp. 449-

464.

9.   Seed, H. B., and Whitman, R. V. (1970). "Design of Earth Retaining Structures for

Dynamic Loads," *Proceedings,* Specialty Conference on Lateral Stresses in the Ground

and Design of Earth Retaining Structures, ASCE, 103-147.

10. Sherif, M. A., Fang, Y. S., and Sherif, R. I. (1984). "K_a and K_0 Behind Rotating and

Non-Yielding Walls," *J. of Geotech. Engrg.*, ASCE, (110)1, pp. 41-56.

11. Sherif, M. A., Ishibashi, I., and Do Lee, Chong (1982). "Earth Pressures Against Rigid Retaining Walls," *J. of Geotech. Engrg.*, ASCE, (108)5, pp. 679-695.

12. Winterkorn, H. F., and Hsai-Yang, F. (1975). Foundation Engineering Hanbook, Van Nostrand Reinhold Co., New York, N. Y., Chapter 5, by Á. Kézdi, pp. 199 and 200

13. Wood, J. H. (1973). "Earthquake-Induced Soil Pressures on Structures," *Report No. EERL 73-05,* Earthquake Engineering Research Laboratories, California Institute of Technology, Pasadena, Calif.

14. Engineering and Design – Retaining and Flood Walls – US Army Corps of Engineers Publication Number: EM 1110-2-2502, 29 September 1989, pp 3-11

Appendix II.- Notation

The following symbols are used in this paper:

α = angle of the failure wedge, or of failure a slice, with the horizontal;

α_0 = slice wedge angle with the horizontal at start of first slip surface at $x = 0$;

α_m = slice wedge angle with the horizontal at end of second slip surface;

β = ramp angle or the slope of the top surface of the wall relative to the x-axis;

δ = Coulomb friction, directional frictional angle between dE_x and dE_y, also it is the

   used as the directional angle for the resultant on a slanted wall, or on a

   vertical wall, relative to a line perpendicular to the wall;

δ_0 = directional angle at first slice boundary at $x = 0$ = incipient shear angle;

δ_m = directional angle at last slice boundary at $x = x_m$ = incipient shear angle;

δ_n = directional angle at slice boundary at $x = x_n$;

δ_E = directional angle for the seismic resultant relative to a line perpendicular to the slanted wall;

C_{IE} = the wall inertia factor;

E_{0r} = at rest horizontal force for a vertical wall with a ramp on top;

E_{0s} = at rest horizontal force for a slanted wall with a ramp on top;

E_{0sE} = at rest horizontal seismic force for a slanted wall with a ramp on top;

$E_{0sE,oc}$ = at rest horizontal seismic force for consolidation for a slanted wall with a ramp on top;

E_{mr} = horizontal force of last slice boundary at $x = x_m$;

E_{nr} = horizontal force of slice boundary at $x = x_n$;

E_r = $E_{0r}(\beta)/\tan\beta$;

E_s = at rest resultant force for a slanted wall with a ramp on top;

E_{rE} = at rest resultant seismic force for a slanted wall with a ramp on top;

dE_x = slice horizontal resultant force;

dE_y = slice vertical resultant force;

ϕ = angle of internal friction of soil;

ϕ' = immobile angle of internal friction of soil;

ϕ_b = friction angle between bottom of the wall and the soil on which it is resting;

ϕ_L = angle of internal friction of soil at loosest state or initial state;

γ = soil unit weight;

γ_D = unit weight of soil at dense state, or actual state, or at rebound state;

γ_L = unit weight of soil at loosest state or initial state;

h = height of wall;

k_h = horizontal acceleration coefficient;

k_v = vertical acceleration coefficient;

K = coefficient of horizontal earth pressure;

K_0 = coefficient horizontal earth pressure at rest for a vertical wall with a flat surface

on top;

$K_{0,oc}$ = coefficient of horizontal earth pressure at rest for overconsolidation for a

vertical wall with a flat surface on top;

K_{0max} = coefficient of seismic horizontal earth pressure at rest for maximum inertia

force;

K_{0r} = coefficient horizontal earth pressure at rest for a vertical wall with a ramp on

top;

$K_{0r}(\beta)$ = same as K_{0r} but used as a function of β;

$K_{0r,oc}$ = coefficient horizontal earth pressure at rest for overconsolidation for a vertical

wall with a ramp on top;

K_{0s} = coefficient of horizontal earth pressure at rest for a slanted wall with a ramp

on

top;

K_{0sE} = coefficient of seismic horizontal earth pressure at rest for a slanted wall with

a ramp on top;

K_{0sEv} = coefficient of seismic vertical earth pressure at rest for a slanted wall with

      a ramp on top;

$K_{0sE,oc}$ = coefficient of seismic horizontal earth pressure at rest for overconsolidation

for

      a slanted wall with a ramp on top;

K_A = coefficient of active earth pressure;

K_{Ah} = coefficient of horizontal active earth pressure;

K_{AE} = coefficient of seismic earth pressure in active condition;

Q = reactive force on bottom of wedge to maintain equilibrium;

dQ = reactive force on bottom of failure wedge or slice to maintain equilibrium;

θ $= \tan^{-1}\left[k_h / (1 - k_v)\right]$;

T = incipient shear vertical force at $x = 0$;

T_m = vertical force of last slice boundary at $x = x_m$;

T_n = vertical force of slice boundary at $x = x_n$;

u $= y + x \tan\beta$;

du $= dy + dx \tan\beta$;

u' $= du/dx = y' + \tan\beta$;

u_0 $= y_0$;

u_m $= y_m + x_m \tan\beta$;

u_n $= y_n + x_n \tan\beta$;

V_{0sE} = at rest vertical seismic force for a slanted wall with a ramp on top;

W = vertical force from weight of wedge;

dW = weight of slice;

W_w = the self-weight of the retaining wall;

ξ = slant angle or the slope of the wall relative to a vertical line or the *y*-axis.

x = coordinate *x*-axis;

dx = width of slice's wedge or the change in x;

x_m = distance to tip of the second slip surface;

x_n = distance to tip of the first slip surface or the start of the second slip surface;

y = coordinate height at *y*-axis;

dy = the change in y;

$d\bar{y}$ = height of slice's wedge;

y' = dy/dx;

y_0 = height of wall or start of first slip surface at $x = 0$;

y_m = height distance at end of second slip surface; and

y_n = height distance at end of first slip surface or start of second slip surface;